
How did the ecological civilization policy rebuild the Human-Water Relationships in the 600-year old “Tunpu” area, China?

Shengtian Yang¹, Zihao Pan¹, Hezhen Lou^{1,*}, Chaojun Li¹,

Jun Zhang¹, Yujia Zhang¹, Yin Yi², Jiye Gong², Ya Luo³, Xi Li³

(1. College of Water Science, Beijing Normal University, Beijing 100875, China;

2. School of Life Sciences, Guizhou Normal University, Guiyang, Guizhou, 550025, China;

3. School of Geographic and Environmental Sciences, Guizhou Normal University, Guiyang 550025, China)

*Correspondence to: Hezhen Lou (11112019051@bnu.edu.cn)

Abstract: With the intensification of climate change and population growth, human-water relationships (HWR) have changed from the simple utilization of water resources to changing the spatial distributions and distribution proportions of water resources through formulating corresponding policies, such as Chinese ecological civilization policy. However, the impact of the ecological civilization policy on the evolution of HWR is still unclear. Here, taking the 600-year old “Tunpu” area as a typical study area, this research analyses the evolution of HWR over different space and time spans based on the Remote Sensing Hydrological Station (RSHS) technology, an improved water balance formula and the transition theory. The results show that at the village scale, the water cycle structure of a typical village has remained stable, and deforestation has increased the proportion of runoff to precipitation by 10.62%. At the basin scale, due to land use/cover changes and precipitation fluctuations, the trend of the runoff changes from slowly decreasing to accelerated increases, with change rate increasing from $-0.073 \times 10^4 \text{ m}^3 \cdot \text{a}^{-1}$ in the Ming Dynasty (1470-1636) to $30.946 \times 10^4 \text{ m}^3 \cdot \text{a}^{-1}$ in the China stage (1949-2020). HWR have developed from the initial balanced resource-rich period to the unbalanced extensive-development period and have finally changed into a rebalancing period under the influence of the ecological civilization policy. Four stages of HWR are as follows: predevelopment (1470-1685), take off (1685-1912), acceleration (1912-2000) and rebalancing (2000-2020). This research indicates that the ecological civilization policy can rebuild HWR, and it is expected to provide enlightenment for future construction of the ecological civilization.

Keywords: Socio-hydrology; Human-Water Relationships; Reconstruction of water cycle; Remote sensing; Ecological civilization.

1 Introduction

Human-water relationships (HWR) have changed from the simple utilization of water resources to changing the spatial distributions and distribution proportions of water resources through formulating corresponding policies because of the

intensification of climate change and population growth (Li et al., 2020). For example, to change the relationship between China's existing development model and the ecological environment, the Chinese government officially put forward the “ecological civilization” policy in 2007 (Hansen et al., 2018; Zhang et al., 2018). To date, the ecological civilization has become the basic ideological framework for China to develop stricter environmental policies (Zhang et al., 2018) and has had a significant impact on China's society, citizens and national policies (Pan, 2012; Xiao and Zhao, 2017; Sha and Iop, 2018; Lu et al., 2019). Due to the important role of water in ecosystem stability and supporting human development (Falkenmark, 2001; Ceola et al., 2016), the “water ecological civilization” has always been an important part of the ecological civilization society (Li et al., 2020). Its purpose is to solve the shortage of water resources, deterioration of the water environment and other water problems that are caused by socioeconomic development, so as to make human and water systems develop harmoniously, which lead to the construction of the ecological civilization that will inevitably affect HWR (Liu and Wang, 2018; Tian et al., 2021). However, most of the studies on the water ecological civilization focus on constructing an evaluation index system, and most of the indicators mainly consist of changes in water systems (Li et al., 2020; Tian et al., 2021; Q. Yang et al., 2021). The impact of major ecological policies, e.g., the ecological civilization, on the evolution of HWR is still unclear.

Currently, studies on the evolution of HWR (Ahmad et al., 2018; Bao and Zou, 2018; Zhao et al., 2020; Zuo et al., 2020; Zuo et al., 2021) are abundant, especially for those countries and areas with a long history of water resource development. The great changes in the natural and social environments will significantly affect the evolution of HWR, which can help us to understand the processes of water problems and are of great significance for improving the understanding of HWR in the past and accurately predicting their possible future dynamics (Sivapalan et al., 2012; Liu et al., 2014; Liu et al., 2015). Therefore, to overcome the limitations of studies with short-time spans that rely on detailed statistical data, some scholars have used the historical literature and hydrological methods to study the evolution of HWR over a span of more than one thousand years in the Tarim River Basin (Liu et al., 2014), Heihe River Basin (Lu et al., 2015), Loess Plateau of China (Wu et al., 2020) and whole China (Wang et al., 2017). The above studies that analyse the evolution of HWR over long periods mainly express the changes in water systems in HWR by using indicators such as temperature, dry and wet climate or precipitation. In addition, runoff is also an important part of the water cycle process, and its amounts are affected by many factors, such as precipitation, temperature and land use/cover change (LUCC), which more directly reflect the evolution of HWR. Due to the difficulty of obtaining runoff data from historical periods, there are few studies on the evolution of HWR over long periods from the perspective of runoff or water cycle processes (Lu et al., 2015).

Many areas of the world have realized the utilization of water resources and live in human-water harmony as early as thousands of years ago. For example, in 793 AD, Charlemagne the Great of the Frankish Kingdom decided to connect the Rhine/Main catchment and Danube catchment by constructing a canal known as the Fossa Carolina, and it could be used for

navigation, irrigation, flood diversion, drainage and water supplies (Leitholdt et al., 2012). In the middle reach of the Mingjiang River in Sichuan Province, China, the Dujiang Dam was initiated during the Qin Dynasty in 256 BC and has been playing the roles of flood control and irrigation for more than 2000 years (Li and Xu, 2006). Besides, there is such a “Tunpu” area in China's experimental ecological civilization area, Guizhou Province, which has its own unique culture and a 600-year history of water resources development, which makes the “Tunpu” area suitable for studying the evolution of HWR over long periods. In 1902, the Japanese scholar, Torii Ryuzo, first discovered the “Tunpu” area and found that as far back as 600 years ago, the “Tunpu” area was inhabited by immigrants who were of Han nationality rather than of Miao nationality, who formed a precious and characteristic “Tunpu” culture (Nie, 2017). Due to the advanced farming technology and ability to build water conservation projects of the Han nationality immigrants, the “Tunpu” people could make full and efficient use of their water resources, which included irrigating paddy fields at different altitudes, effectively resisting drought and flood discharges, and providing domestic water and hydropower for the entire village (Zhang and Pang, 2007).

Therefore, taking the “Tunpu” area as a typical study area, based on the Remote Sensing Hydrological Station (RSHS) technology and an improved water balance formula, we tried to find significant implications from the HWR in this famous area, the main study contents of this research include the following three points: (1) The historical and modern water cycle processes at the village scale are reconstructed; (2) Then 600 years’ LUCC was also retrieved by using remote sensing and historical data, and the water cycle processes at the basin scale are reconstructed over the past 600 years. (3) Based on transition theory, the key time nodes of the evolution of HWR are determined, and the impact of the ecological civilization on HWR is analysed.

2 Study area

The “Tunpu” area, with a 600-year history of water resource development, is located in Anshun city, Guizhou Province, which is an experimental ecological civilization area in China (105.975°E - 106.366°E, 26.159°N - 26.463°N). The “Tunpu” area is mainly located in the Yangchang River Basin, which belongs to the Wujiang River System in the Yangtze River Basin, with a drainage area of 721.78 km². The basin has a north subtropical monsoon humid climate, with an annual average temperature of 14-15°C and annual precipitation of 1200-1300 mm. The presence of karst development, poor water holding capacity and high surface water permeability in the basin cause it to be prone to soil erosion and rocky desertification (Fig. 1a).

In view of the history of water resource development and utilization and the modern ecological civilization policies in the “Tunpu” area, it is suitable for studying the evolution process of HWR over a long period. As early as 1382, the “Tunpu” area was inhabited by many Han immigrants who came from the south part of the Yangtze River and from the Central Plains, who were clearly different from the surrounding ethnic minorities and Han nationalities in their clothing, language,

architecture, customs and culture, forming a precious and characteristic “Tunpu” culture (Fig. 1a). Moreover, through the construction of water conservancy projects such as backwater weirs, “fish mouth water diversion”, water-powered rollers and water mills in “Baojia Tun” (Fig. 1b and Fig. 1c), the “Tunpu” people were able to achieve the efficient utilization of water resources and live in human-water harmony as far back as 600 years ago. In modern times, when facing the severe situation of tight resource constraints, serious environmental pollution and ecosystem degradation that were caused by accelerated socioeconomic development, Guizhou Province, where the “Tunpu” area is located, the area has actively responded to the call of the state and has implemented the construction of the ecological civilization. After 2000, key projects for the prevention and control of soil erosion were launched, and ecological construction projects focusing on returning farmlands to forests were vigorously promoted. After 2005, this area took the lead in making the strategic decision of building the ecological civilization and was established as a national ecological civilization experimental area (Jiang et al., 2014).

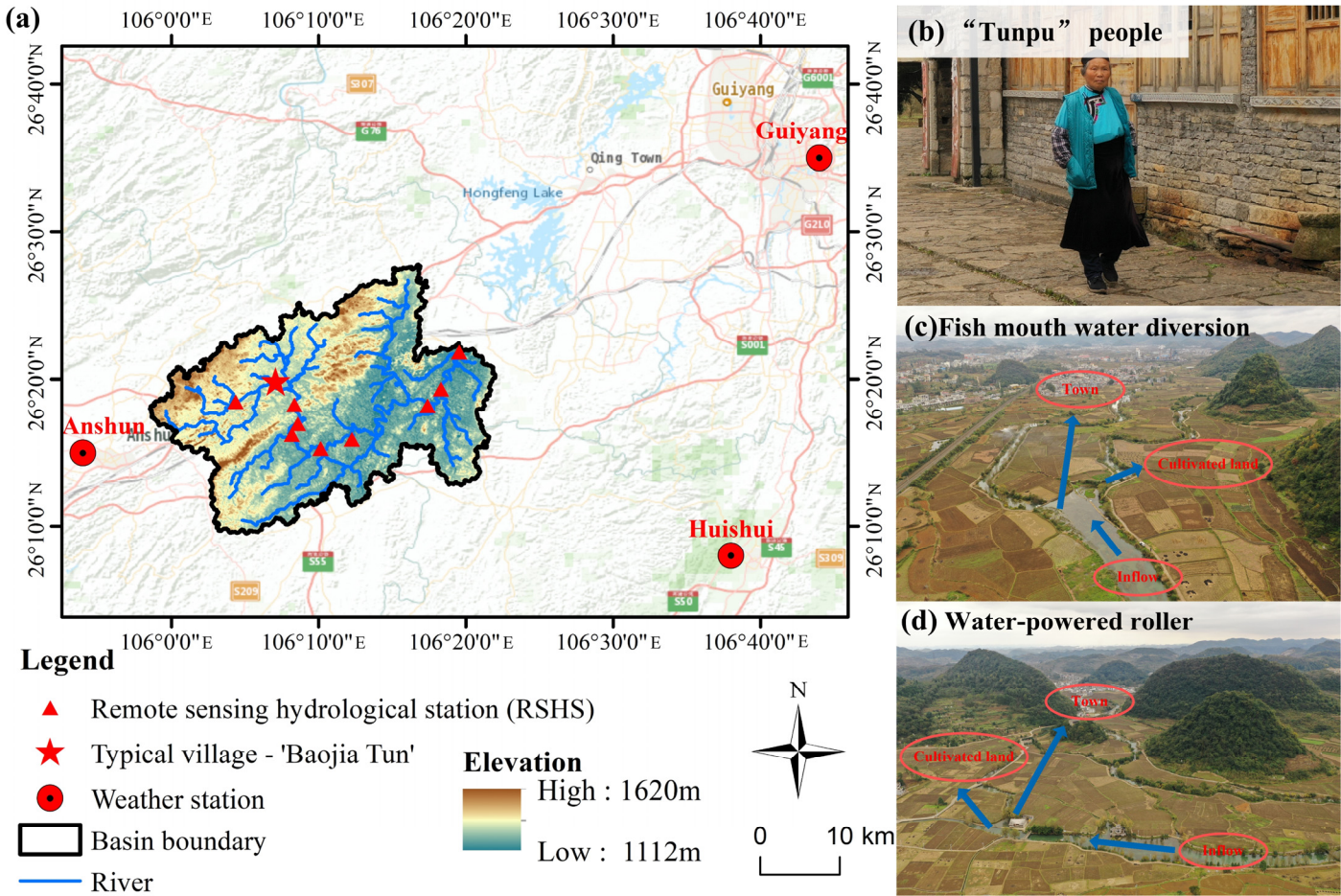


Figure 1. (a) Study area of this research; (b) the “Tunpu” people wear traditional costumes; (c) “Fish mouth water diversion” of “Baojia Tun”; and (d) water powered roller of “Baojia Tun”.

3 Methods and data

(1) Reconstruction of the water cycle process at the village scale

An improved water balance formula that considers irrigation water and domestic water is constructed. The formulas are as follows:

$$\begin{cases} P - ET - \Delta W - DW = R \\ I - \Delta ET_{paddy} = IB \end{cases} \quad (1)$$

where P is precipitation, m^3 ; ET is the actual evapotranspiration, m^3 ; ΔW is the water storage variable of the basin, which can be regarded as 0; DW refers to the total domestic water consumption, $100 \text{ L} \cdot (\text{capita} \cdot \text{day})^{-1}$; R is the total runoff, m^3 ; I and IB are the irrigation water and irrigation backwater amounts, m^3 , respectively, and ΔET_{paddy} is the difference between evapotranspiration with irrigation and that without irrigation, m^3 .

To analyse the changes in the water cycle structure and its elements and by assuming that the precipitation is 100%, it is only necessary to reconstruct the evapotranspiration sequence according to the land use/cover data of the two periods, and the changes in runoff can then be obtained. To calculate the evapotranspiration, the formula for calculating the actual evapotranspiration is based on the Budyko hypothesis that was proposed by Fu (1981). In addition, cultivated lands are divided into paddy fields and dry lands, and the water sources for the evapotranspiration from paddy fields include not only precipitation but also irrigation water. The formulas are as follows:

$$\frac{ET}{P} = 1 + \frac{ET_0}{P} - [1 + (\frac{ET_0}{P})^w]^{1/w} \quad (2)$$

$$P_{paddy} = P + I \quad (3)$$

where ET_0 is the potential evapotranspiration, m^3 ; w is the basin-scale model parameter; and w was defined as 3.5 for all land use/cover types in the arid basin, which is not applicable to the study of humid basins. Therefore, the values of w for forestland, cultivated land, grassland and construction land are defined as 2.25, 1.7, 1.55 and 1.35, respectively; P_{paddy} is the quantity of water resources that can be used for evapotranspiration in paddy fields, m^3 ; I is the irrigation water amount, and the irrigation quota is $795 \text{ mm} \cdot \text{a}^{-1}$.

(2) Reconstruction of the water cycle process at the basin scale

The water balance formula of reconstructing basin scale water cycle process is basically the same as that of village scale, and the measured surface runoff data can be used to analyse the reliability of the runoff calculated by water balance formula. Due to the small size of the basin and lack of continuous hydrological observation data, the RSHS technology can be used to address the difficulty of obtaining surface runoff data in ungauged basins (Yang et al., 2019; Zhao et al., 2019; Lou et al., 2020; Wang et al., 2020; Yang et al., 2020; Wufu et al., 2021; S. Yang et al., 2021). The RSHS method uses an unmanned aerial vehicle to assist the field survey in generating a digital river model with terrain data accuracies as small as the centimetre level. Then, the long-time series of the river width data can be inverted according to satellite remote sensing Normalized Difference Water Index (NDWI) data and the sub-pixel decomposition method (formula 4). Finally, based on the Manning formula, the long-time series of the surface runoff data can be estimated by calculating hydraulic parameters such

as overflow area, hydraulic radius and wetted perimeter length to a specific river width (formula 5).

$$W = \sum_{i=1}^x \begin{cases} \frac{PA}{VL} & NDWI^i > NDWI_{WT} \\ \left(\frac{NDWI^i - NDWI_{LT}}{NDWI_{WT} - NDWI_{LT}} \right) * \frac{PA}{VL} & NDWI_{LT} < NDWI^i < NDWI_{WT} \\ 0 & NDWI^i < NDWI_{LT} \end{cases} \quad (4)$$

$$\begin{cases} R'(W) = V \times A = \frac{k}{n} \times HR^{2/3} \times J^{1/2} \times A \\ HR = L/A \end{cases} \quad (5)$$

where W is the average river width of the selected river valley, m; x is the total number of pixels in the selected river valley; $NDWI^i$ is the $NDWI$ of pixel i ; $NDWI_{LT}$ and $NDWI_{WT}$ are the $NDWI$ threshold of land and water, respectively; PA is the area of each pixel, m^2 ; VL is the length of the selected river valley, m; $R'(W)$ is the estimated runoff corresponding to river width W , m^3 ; V is the flow velocity, $m \cdot s^{-1}$; k is the conversion constant, $k = 1$; n is the roughness, which comprehensively reflects the impacts of the river channel roughness on river flow, $n = 0.035$; HR is the hydraulic radius, m; J is the slope, measured by UAV remote sensing image; L is the Wetted perimeter length, m; A is the overflow area, m^2 ; L is the wetted perimeter length, m; HR , L , and A are calculated by river width and digital river model.

However, different from the reconstruction of the water cycle process at the village scale, it is necessary to consider climate change and reconstruct the precipitation sequence year by year at the basin scale. *The atlas of drought and flood distribution in China in the past 500 years* systematically reproduces the general characteristics of the annual drought and flood distributions for the 531 years from 1470-2000 (Institute of Meteorological Sciences, 1981; Zhang and liu, 1993; Zhang et al., 2003), and the rationality of this atlas is shown by its application in the Heihe River Basin and other regions (Ren et al., 2010; Lu et al., 2015). After determining the drought and flood levels in the basin from 1470 to 2000 by using the atlas, the precipitation levels for the basin area according to the measured precipitation data of the national meteorological stations from 1959 to 2000 are calculated, and the annual precipitation anomaly percentages that correspond to each drought and flood level within an appropriate range are then determined (Table 1). In addition, the intensity of the East Asian monsoon is one of the main factors that affects the precipitation in the basin, and the study area also experienced a small ice age (1470-1633), strong monsoon period (1634-1950) and weak monsoon period (1951-2020) from 1470 to 2020 (Cai et al., 2001; Zhao, 2011).

Table 1. Precipitation corresponding to drought and flood levels.

drought and flood level	Description	Annual Precipitation Anomaly Percentage (Feasible range) (%)	Annual Precipitation(mm)
1 (Flooding)	Precipitation with long duration and high intensity, large-scale flood, and severe typhoon disasters along the coast	25 (10 ~ 30)	1439.29
2 (Partial flooding)	Continuous precipitation with less severe disasters, local flood, hurricane and heavy rain with less severe disasters in a single season	10 (5 ~ 10)	1273.22
3 (Normal)	Harvest or no record	0 (-5 ~ 5)	1107.15
4 (Partial drought)	Drought and local areas with minor disasters in a single season and	10 (-10 ~ -5)	941.07

	month		
5 (Drought)	Continuous drought for several months or cross quarter drought, large-scale severe drought	-25 (-30 ~ -10)	775.00

Besides, the method for calculating the evapotranspiration is generally the same as that for the village scale, and only the part that obtains the land use/cover data is different. The LUCC before 1980 consisted mainly of transformations of cultivated land and forestland (Pan, 2021), so if the changes in cultivated land areas are compiled, the land use/cover data in the historical period can be reconstructed. In addition, the spatial distribution of LUCC is of great significance for studying the evolution of HWR, and an index called the cultivated land expansion index is constructed to reflect the sequence of cultivated land expansion. The formulas are as follows:

$$\begin{cases} CLEI = \alpha_1 NHD + \alpha_2 NRD + \alpha_3 NS \\ NHD = HD / (HD_{MAX} - HD_{MIN}) \\ NRD = RD / (RD_{MAX} - RD_{MIN}) \\ AS = \begin{cases} 0 & 0 \leq S \leq 0.25 \\ 1 & 0.25 < S \leq 1 \end{cases} \end{cases} \quad (6)$$

where $CLEI$ is the cultivated land expansion index, $CLEI \in [0,1]$; the closer $CLEI$ is to 0, the more likely this pixel is to be developed into cultivated land earlier; NHD , NRD and AS are the normalized habitation distance, normalized river distance and adjusted slope, respectively; α_1 , α_2 and α_3 are weight coefficients, $\alpha_1 = \alpha_2 = \alpha_3 = 1/3$; HD , RD and S are the habitation distance, river distance and slope of one pixel, respectively; and HD_{MAX} , HD_{MIN} , RD_{MAX} and RD_{MIN} are the maximum habitation distance, minimum habitation distance, maximum river distance and minimum river distance of the whole basin, respectively, m.

(3) Key time nodes of the evolution of HWR

Transition theory is one of the most relevant methods to understand the evolution of socioeconomic systems and support sustainable development management (Tàbara and Ilhan, 2008; Lu et al., 2015). In this research, the per capita water resources, human water consumption, forestland areas and populations are selected as indicators to understand the evolution of the HWR in the Yangchang River basin over the past 600 years. Among these indicators, the per capita water resources reflect the changes in the background conditions of water resources. Human water consumption reflects the impact of socioeconomic development on the water cycle process. The forestland area reflects the eco-environmental quality and water conservation capacity. The population reflects the degree of socioeconomic development. Finally, according to the directions and rates of change of these four indicators, the HWR can be divided into four different development stages, namely, predevelopment, take-off, acceleration and rebalancing. The formulas are as follows:

$$\begin{cases} PCWR = R/POP \\ HWC = I + DW \end{cases} \quad (7)$$

where $PCWR$ is the per capita water resources, m^3 per capital; POP is the population; and HWC is the total human water consumption, m^3 .

(4) Data collection and processing

Three types of data are collected and used to analyse the evolution of HWR (Table 2). The first category is land use/cover data. At the village scale, the historical land use/cover data are determined by using the restored map of “Baojia Tun” (Zhou and Xu, 2018), and the modern land use/cover data are determined by using the 2020 global 30-m land use/cover data and unmanned aerial vehicle remote sensing images that were obtained by a DJI Mavic Air 2 drone. At the basin scale, the land use/cover data for the historical period consist of the cultivated land areas in the study area that were sorted and estimated from the relevant documents describing the agricultural development in Guizhou Province and Anshun city. From 1980-2020, the China multi-period 30-m land use/cover remote sensing monitoring dataset will be used, and the years without data will directly use the land use/cover data from the closest year. The second category consists of the data that are used to reconstruct the precipitation and evapotranspiration levels in the water cycle process. The precipitation amounts are determined by the drought and flood levels for the period from 1470 to 2000. Based on the measured precipitation data from meteorological stations from 1958 to 2000, the correlation between these data and the drought and flood levels can be established. For the precipitation data obtained from meteorological stations from 2001 to 2020, the inverse distance weight method will be used to calculate the area precipitation levels. The Moderate-resolution Imaging Spectroradiometer (MODIS) Terra Net Evapotranspiration product (MOD16A2.006) in the Google Earth Engine is processed to provide the annual average potential evapotranspiration and actual evapotranspiration levels for the Yangchang River basin. The third category consists of data that are used to analyse the evolution of HWR, which include population changes, per capita domestic water consumption levels, and irrigation quotas, which are obtained from the literature and statistical data.

Table 2. Data sources.

Data name	Date range	Purpose	Source
Restored map of “Baojia Tun”	The Ming dynasty	Reconstruct land use/cover at the village scale	(Zhou and Xu, 2018)
Global 30 m land use/cover data	2020		National Geomatics Center of China
Cultivated land area in historical period	1470-1980	Reconstruct land use/cover at the basin scale	(Zhang, 1998; Xue et al., 2014; Chen, 2016)
China multi period land use and land cover remote sensing monitoring dataset (CNLUCC) (30 metres)	1980, 1990, 2000, 2005,		(Xu et al., 2018)
Atlas of drought and flood distribution in China in recent 500 years	1470-2000	Reconstruct precipitation	(Institute of Meteorological Sciences, 1981; Zhang and liu, 1993; Zhang et al., 2016)
Precipitation data of meteorological stations	1958-2020		China Meteorological Data Network(http://data.cma.cn)
MOD16A2.006 Terra Net Evapotranspiration (500 metres)	2001-2020	Reconstruct evapotranspiration	GEE
Unmanned aerial vehicle low altitude remote sensing (<1 m)	2020		DJI Mavic Air 2

Landsat-7, Landsat-8 and Sentinel-2 Surface reflectance	2001-2020	Remote sensing hydrological	GEE
Population in historical period	1470-2000	Analyse the evolution of HWR	(Jiang, 1982; Yang, 1996; Zhang, 1998; Chen, 2016)
Statistical Bulletin of National Economic and Social	2001-2020		China Statistical Information
China City Statistical Yearbook	2001-2020		China Statistics Press
Water Resources Bulletin of Anshun City	2008-2019		Anshun Water Resources Bureau(http://swj.anshun.gov.cn/)
Statistical Yearbook of Anshun City	2012-2019		Anshun Municipal Bureau of Statistics(http://www.anshun.gov.cn/zfsj)

4 Results

4.1 Water cycle process at the village scale over the past 600 years

Water cycle processes during the Ming Dynasty (1470-1636) and modern times (2020) at the village scale are analysed (Fig. 2). Fig. 2 shows that with continuous socioeconomic development, the population of “Baojia Tun” has increased from 529 to 2870, but the water cycle structure in “Baojia Tun” has generally remained stable. The socioeconomic development model still represents a small-scale peasant economy, and the human impacts on the water cycle process are still dominated by irrigation water; only the precipitation percentages that are accounted for by various elements in the water cycle process have changed.

For the evapotranspiration, the cumulative evapotranspiration accounted for 73.66% of precipitation during the Ming Dynasty, of which the evapotranspiration levels of forest and grassland (36.21%) and cultivated land were similar (35.64%), while the evapotranspiration level of construction land was very small (1.81%). In modern times, due to the expansion of cities and towns and cultivated land, large amounts of deforestation have occurred, and the forestland area has been reduced from 0.262 km² to 0.072 km². As a result, the evapotranspiration levels of cultivated land and construction land have increased to 43.66% and 9.82%, respectively, the evapotranspiration level of forest and grassland has decreased sharply to 9.43%, and the total evapotranspiration has also decreased to 62.91%. Regarding the impacts of human activities on the water cycle process, the irrigation water consumption has increased from 35.90% to 43.97%, and the amount of irrigation return water has also increased from 27.42% to 33.59%. Although the proportion of domestic water consumption in precipitation is very small, its range of increase is as high as 542.55%. The last factor is runoff. Because forestland is the most important water conservation land use/cover type, the deforestation of forestland has led to runoff increases that range from 26.31% to 36.93%. Although the total runoff has increased significantly, the surface runoff will not increase significantly due to the simultaneous increase in irrigation water levels, which will lead to more surface runoff being converted into interflow or underground runoff.

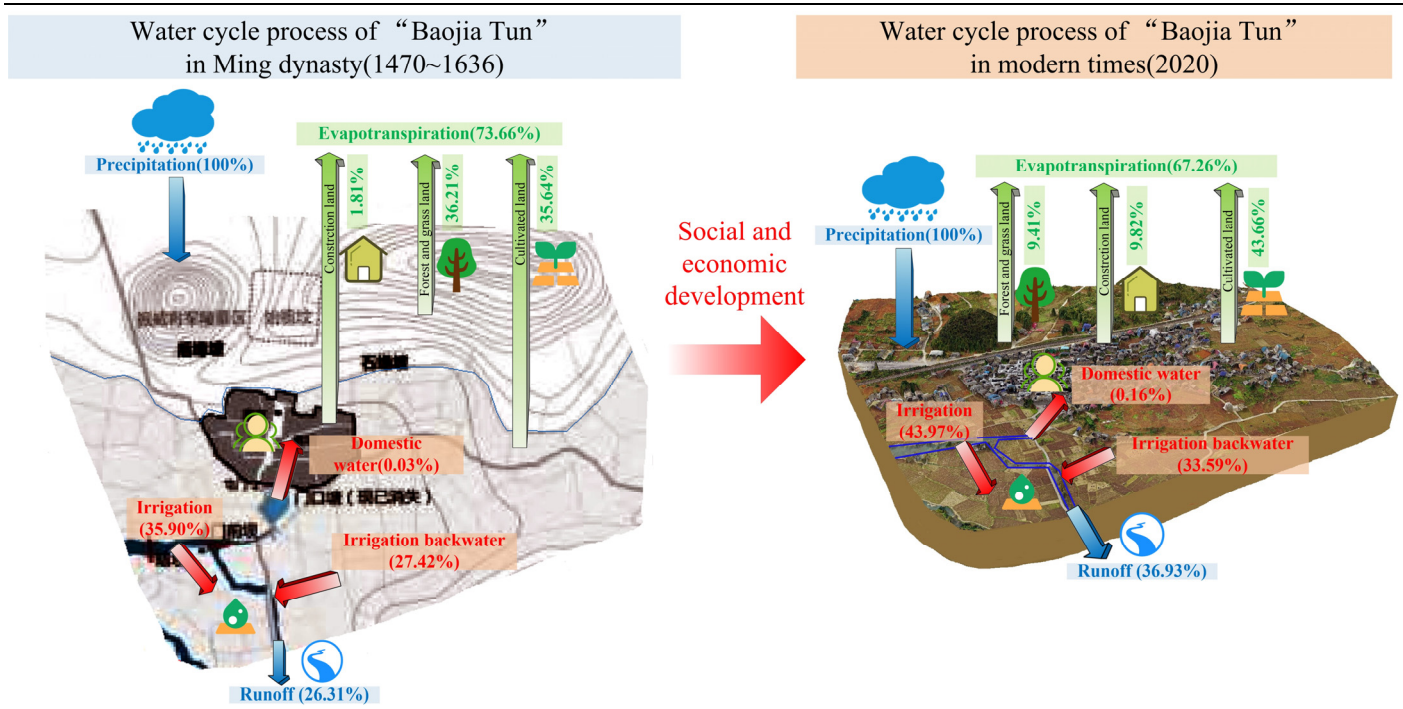


Figure 2. The change of water cycle processes in “Baojia Tun” from the Ming Dynasty to modern times.

4.2 Variations in water resources at the basin scale over the past 600 years

By using correction coefficients of 0.9 and 1.1 for the precipitation during the Little Ice Age (1470-1633) and strong monsoon period (1634-1950), respectively, the precipitation, evapotranspiration and runoff time series from 1470 to 2020 are reconstructed at the basin scale (Fig. 3a). RSHS and the measured precipitation of the weather station was used to verify the accuracy of the reconstructed runoff and precipitation, respectively, the variation result of precipitation and runoff can be seen in supplementary Fig.1. Under the joint influence of precipitation and evapotranspiration, the runoff exhibited a significant increasing trend ($P < 0.05$), with an average annual runoff of $2.02 \times 10^8 \text{ m}^3$ from 1470 to 2020 and an overall rate of increase of $8.41 \times 10^4 \text{ m}^3 \cdot \text{a}^{-1}$. Through a further analysis of the changes in the water cycle process in different stages, it can be found that the runoff trend changed from a slow decrease to an accelerated increase, and the rate of change increased from $-0.073 \times 10^4 \text{ m}^3 \cdot \text{a}^{-1}$ in the Ming Dynasty (1470-1636) to $30.946 \times 10^4 \text{ m}^3 \cdot \text{a}^{-1}$ in the China stage (1949-2020) (Fig. 3b). From the Ming Dynasty to the Qing Dynasty (1636-1912), the annual average precipitation, evapotranspiration and runoff levels increased by 0.239 , 0.102 and $0.132 \times 10^8 \text{ m}^3$, respectively, which indicated that the impact of human activities on the water cycle process at this stage was still slight, and the changes in various elements in the water cycle process were mainly caused by the increased precipitation. From the Qing Dynasty to the Republic of China stage (1912-1949), the change mode changed, mainly because large-scale cultivated land development occurred during this stage, and the amount of forestland greatly decreased, which thus decreased the evapotranspiration. As a result, for the condition of an annual average precipitation increase of $0.058 \times 10^8 \text{ m}^3$, the evapotranspiration decreased by $0.051 \times 10^8 \text{ m}^3$ instead, which resulted in an increase in runoff of $0.098 \times 10^8 \text{ m}^3$. In the

Republic of China to China stage (1949-2000), for a condition of an annual average precipitation reduction of $0.227 \times 10^8 \text{ m}^3$, the impact of human activities on the water cycle process remained stable but to a greater extent, which resulted in a $0.491 \times 10^8 \text{ m}^3$ decrease in evapotranspiration and $0.239 \times 10^8 \text{ m}^3$ increase in runoff. From the China (1949-2000) to China (2000-2020) stages, due to the joint impacts of forestland restoration and construction land expansion, the impacts of human activities on the water cycle process have changed, and the reduction in evapotranspiration that is caused by human activities has been suppressed. The annual average precipitation and evapotranspiration levels decreased by 0.009 and $0.103 \times 10^8 \text{ m}^3$, respectively, and the runoff increased by $0.061 \times 10^8 \text{ m}^3$.

Besides, the precipitation exhibited a periodic change trend of "decrease-increase-decrease-increase". Among them, from 1470 to 1633, there was a small ice age with a dry, cold climate, and the average annual precipitation was only $7.84 \times 10^8 \text{ m}^3$ and showed a decreasing trend with a rate of $-1.35 \times 10^4 \text{ m}^3 \cdot \text{a}^{-1}$. From 1634 to 1949, there was a strong monsoon period with a warm, humid climate and average annual precipitation of $8.09 \times 10^8 \text{ m}^3$, and the precipitation during this period exhibited an increasing trend with a rate of $3.48 \times 10^4 \text{ m}^3 \cdot \text{a}^{-1}$. The period from 1950 to 2020 consisted of a weak monsoon period with an average annual precipitation of only $7.90 \times 10^8 \text{ m}^3$. Although there was a small precipitation reduction at the beginning of this period, the precipitation also exhibited an obvious increasing trend with a rate of $16.10 \times 10^4 \text{ m}^3 \cdot \text{a}^{-1}$, which is consistent with the increased precipitation in recent decades that is caused by climate warming.

In addition, the changes in evapotranspiration exhibited a trend of "increase-decrease". From 1470 to 1912, the annual average evapotranspiration was $6.02 \times 10^8 \text{ m}^3$, and the evapotranspiration finally exhibited an obvious increasing trend with a rate of $3.24 \times 10^4 \text{ m}^3 \cdot \text{a}^{-1}$ due to the increased precipitation. However, the proportion of evapotranspiration for cultivated land in the total evapotranspiration gradually increased from 1.27% to 6.52% due to the increased cultivated land area (Fig. 3c). From 1913 to 2020, the average annual evapotranspiration was $5.66 \times 10^8 \text{ m}^3$ and exhibited an obvious decreasing trend with a rate of $-76.78 \times 10^4 \text{ m}^3 \cdot \text{a}^{-1}$. This is because the decrease in evapotranspiration that was caused by human activities was greater than the increase in precipitation, resulting in the rapid increase in the proportion of evapotranspiration of cultivated land and construction land in the total evapotranspiration in this period, which reached maximum values of 48.48% and 1.46% in 2000-2010 and 2010-2020, respectively.

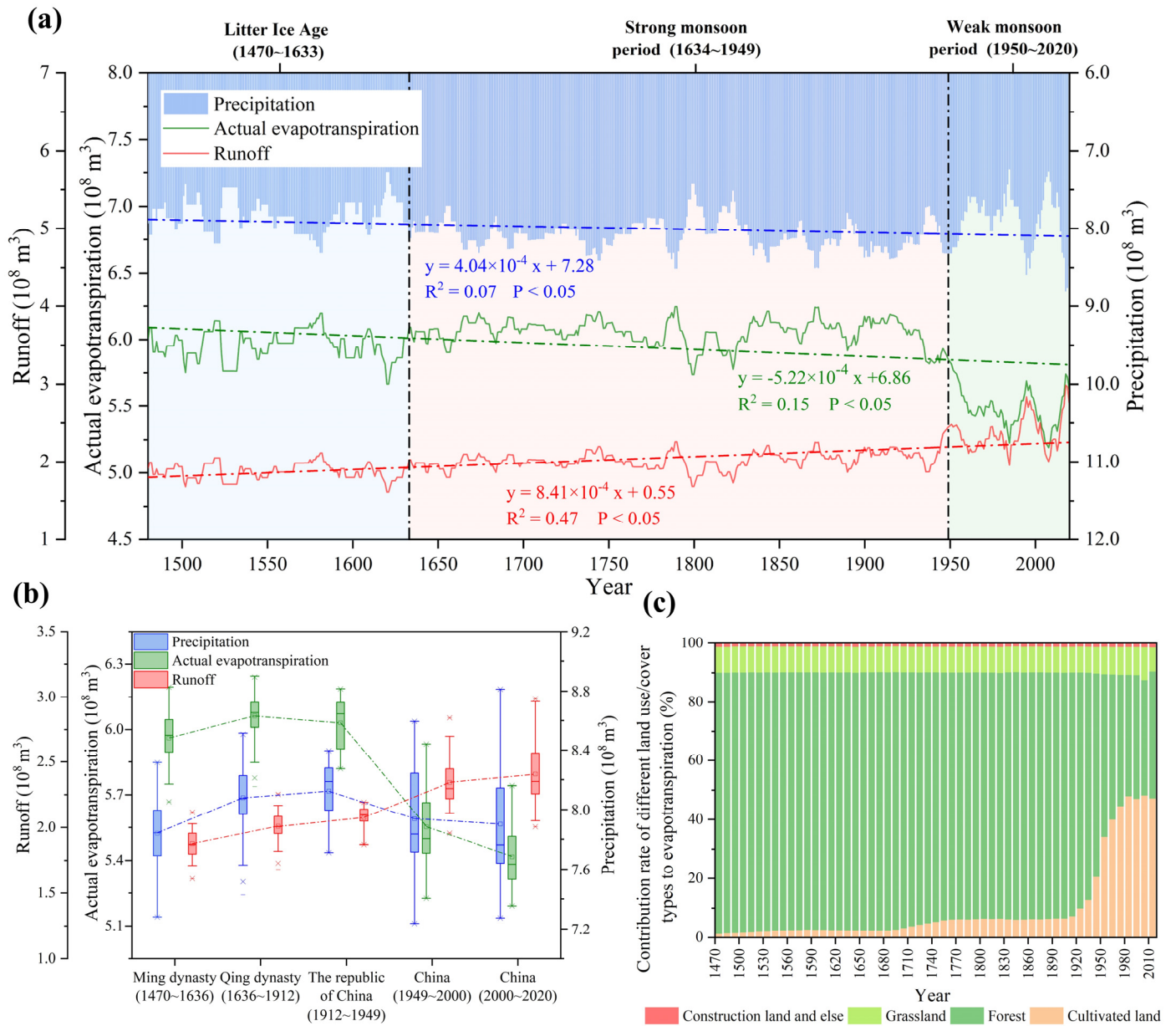


Figure 3. Reconstruction of the water cycle process from 1470 to 2020 at the basin scale. (a) 10-year moving average values of precipitation, evapotranspiration and runoff; (b) changes in the water cycle process in different stages; and (c) changes in composition of the cumulative actual evapotranspiration.

4.3 Human actions in this 600-year area

From 1470 to 1980, human activities were mainly characterised by the expansion of cultivated land, the cultivated land area was classified, and its spatial distribution was estimated (Fig. 4a). Fig. 4a shows that until 1636 (the end of the Ming Dynasty), the maximum cultivated land area was only 20.19 km². By 1912, the end of the Qing Dynasty, the cultivated land area had increased to 49.87 km². After that, the increase in cultivated land area entered an accelerated mode and reached

217.55 km² and 355.51 km² in 1949 and 1980, respectively. To reconstruct the spatial distributions of the cultivated land expansions in the past 600 years and to divide these by periods, the cultivated land expansion index *CLEI* is calculated. The three most appropriate thresholds were selected to cause the cultivated land area in each period to be as close as possible to the literature results, which are 0-0.032 (20.12 km²), 0.032-0.053 (28.49 km²), 0.053-0.162 (169.31 km²) and 0.162-0.855 (137.59 km²), respectively.

From 1980 to 2020, six sets of 30-m land use/cover data obtained from the Chinese Academy of Sciences in 1980, 1990, 2000, 2005, 2010 and 2015 will be used directly, and the years without data will directly use the land use/cover from the closest year (Fig. 4b-d). Fig. 4b-d shows that the LUCC from 1980 to 2020 consisted mainly of the expansion of construction land that was supplemented by a few forestland restoration efforts. Among them, the area of construction land increased slowly from 1980 to 2000 and showed a rapid increasing trend after 2000, from 75.95 km² in 2000 to 216.56 km² in 2015, with an increase of 285.13%. For cultivated land, the area of dry land generally remains stable, while the area of paddy fields continue to decrease, from 245.79 km² to 238.07 km², a decrease of 3.14%. The total area of grassland decreased from 94.93 km² in 1980 to 81.00 km² in 2015, and the total area of forestland increased from 260.88 km² in 2000 to 268.77 km² in 2015.

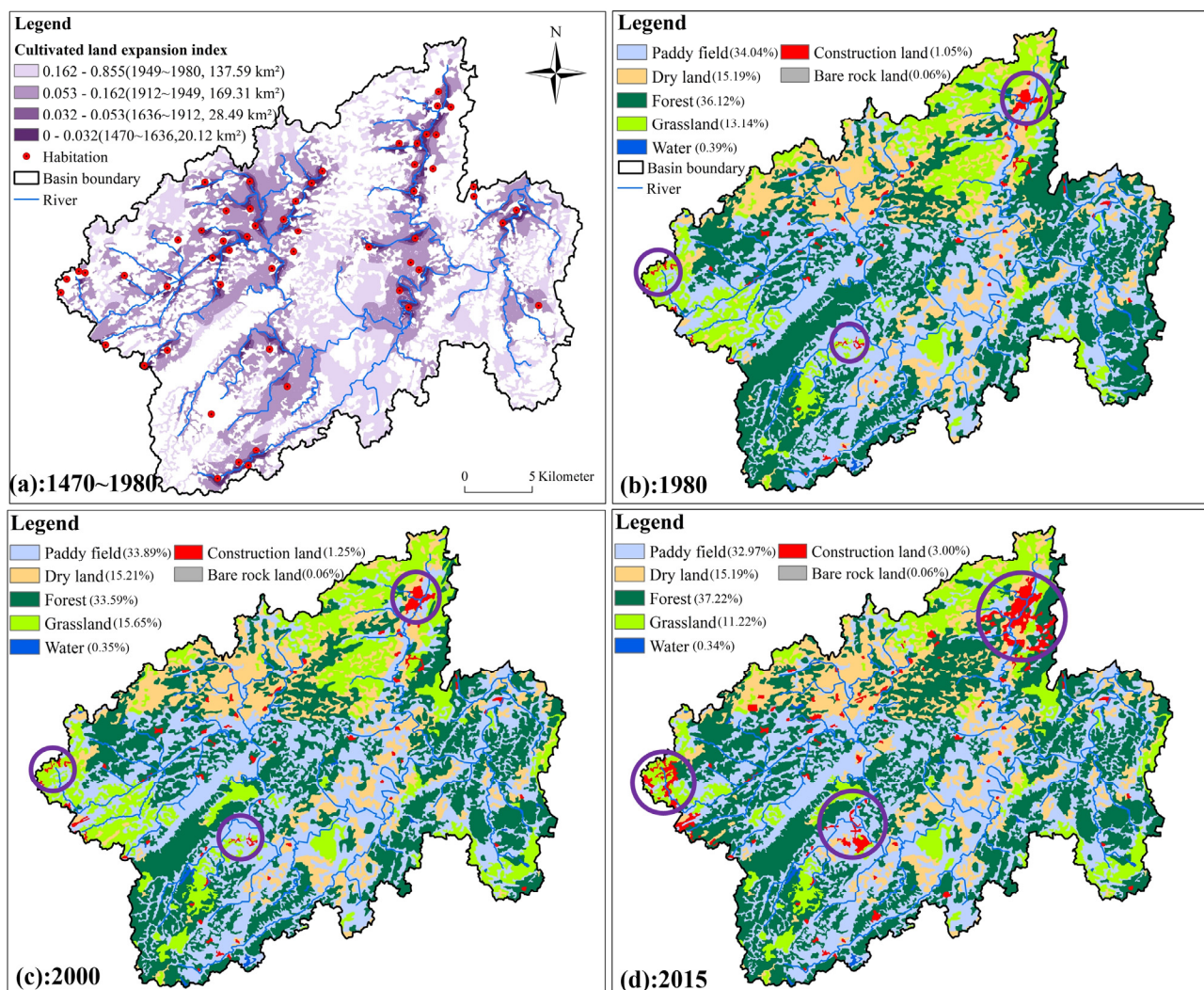


Figure 4. Human actions in the past 600 years. (a) The cultivated land ranges from 1470 to 1980, (b) land use/cover in 1980, (c) land use/cover in 2000, and (d) land use/cover in 2015. The purple circles represent the areas with obvious expansions of construction land, and the circle diameters reflect the scopes of construction land.

4.4 Evolution of HWR at the 600-year scale

Based on transition theory, the change slopes and average per capita values of the water resources, human water consumption, forest areas and population in the Yangchang River Basin from 1470 to 2020 are analysed. The results show that the HWR continued to develop from the initial balanced resource-rich period to an unbalanced period with extensive development and finally to a rebalancing period, which can be divided into the following four stages: predevelopment (1470-1685), take off (1685-1912), acceleration (1912-2000) and rebalancing (2000-2020) (Fig. 5).

The predevelopment stage (1470-1685) occurred from the mid-Ming Dynasty to the early Qing Dynasty. For this stage, the socioeconomic development level of the basin is slow, the water and forest resources are rich, and the overall degree of human development of water resources is low. This stage belongs to a balanced resource-rich period of HWR. In detail, the population growth is slow ($16 \text{ people} \cdot \text{a}^{-1}$), and the per capita water resources exhibit a rapid decreasing trend ($\text{Pcwr}_{k1} = -0.059 \text{ thousand m}^3$) under the influence of precipitation change and population growth. The short period of growth of the per capita water resources was due to the population decline from 1620 to 1637, when there were frequent wars during the change in dynasties (Sheng et al., 2019). However, the per capita water resources are relatively abundant, with an average of $27.50 \text{ thousand m}^3 \cdot (\text{capita} \cdot \text{year})^{-1}$. Although the human water consumption showed an insignificant increasing trend ($\text{Hwc}_{k1} = 0.0003 \times 10^8 \text{ m}^3$), the average annual human water consumption was $0.13 \times 10^8 \text{ m}^3$, which accounted for only 7.04% of the average runoff at this stage. At the same time, the basin was rich in forest resources, with an average forest area of 599.93 km^2 , which accounted for 83% of the total basin area, and the decreasing trend is not obvious ($\text{Fa}_{k1} = -0.92 \text{ km}^2$).

The take-off stage (1685-1912) occurred in the middle and late Qing Dynasty. With the decrease in warfare and gradual stabilisation of society, the level of socioeconomic development begins to increase during this stage, the human impact on the water cycle process is still slight, and the water resources and forest resources are still at relatively rich levels, but the HWR began to shift towards an imbalance. At this stage, the population began to increase ($106 \text{ people} \cdot \text{a}^{-1}$). Although the decline rate of the per capita water resources was slightly lower than that of the predevelopment stage due to the increased precipitation that was caused by the strong monsoon period during this stage ($\text{Pcwr}_{k2} = -0.041 \text{ thousand m}^3$), its average value was $8.70 \text{ thousand m}^3 \cdot (\text{capita} \cdot \text{year})^{-1}$, which was only 31.65% of the value during the predevelopment stage. To meet the food needs of the increased population, the area of cultivated land expanded to a slight extent, which resulted in the increase rate of human water consumption being 300% of that of the predevelopment stage ($\text{Hwc}_{k2} = 0.0009 \times 10^8 \text{ m}^3$), but

its proportion of runoff is only 17.29%. Although the forest resources have decreased slightly, they are still relatively abundant. The forestland area accounts for 79.45% of the total basin area on average, but its reduction rate is 415.22% of that of the predevelopment stage ($Fa_k2 = -3.82 \text{ km}^2$).

The acceleration stage (1912-2000) occurred during the transition from the Republic of China to the new China. Due to the changes in the socioeconomic system and liberation of productive forces, socioeconomic development has accelerated in an extensive manner, the utilization degree of water resources has reached a high level, and the amount of water resources in the basin will have difficulty supporting higher-intensity development. Meanwhile, with the reduction in forestland, the quality of the ecological environment increasingly declined, and the HWR entered an imbalanced stage. At this stage, the population growth rate increased further ($1711 \text{ people} \cdot \text{a}^{-1}$), which resulted in a faster decrease in per capita water resources ($Pcwr_k3 = -0.048 \text{ thousand m}^3$), and the average value decreased to only $2.94 \text{ thousand m}^3 \cdot (\text{capita} \cdot \text{year})^{-1}$. Due to the surge in cultivated land irrigation and human domestic water demand, human water consumption increased rapidly ($Hwc_k3 = 0.0219 \times 10^8 \text{ m}^3$), which accounting for 61.06% of the total runoff on average, and reached a maximum value of 102.69% in 1985. Meanwhile, to provide the necessary land for the expansion of cultivated land and construction land, the forestland area decreased at a very rapid rate ($Fa_k3 = -70.52 \text{ km}^2$) and reached the lowest value of 244.47 km^2 in 1999.

The rebalancing stage (2000-2020) occurred in the China period. Due to the influence of ecological and environmental protection policies such as the ecological civilization, the basin has maintained a rapid level of socioeconomic development but also considers the protection of water resources and restoration of the ecological environment. As a result, the ecological civilization rebuilds HWR and causes them to transition to a rebalancing stage with high consumption and high output. At this stage, the population growth rate reached its highest level ($2737 \text{ people} \cdot \text{a}^{-1}$). Although the average per capita value of water resources has been as low as $1.12 \text{ thousand m}^3 \cdot (\text{capita} \cdot \text{year})^{-1}$, its decreasing trend has been alleviated to some extent ($Pcwr_k4 = -0.006 \text{ thousand m}^3$). Due to the reduced area of cultivated land, human water consumption exhibited a significant decreasing trend after increasing in the first three stages ($Hwc_k4 = -0.0021 \times 10^8 \text{ m}^3$) and accounted for 83.84% of the runoff on average, which means that the Yangchang River basin relied on less water to feed more humans than before. At the same time, the forest area also exhibited an upwards trend for the first time ($Fa_k4 = 1.11 \text{ km}^2$), which also means improved environmental quality and soil and water conservation capacity.

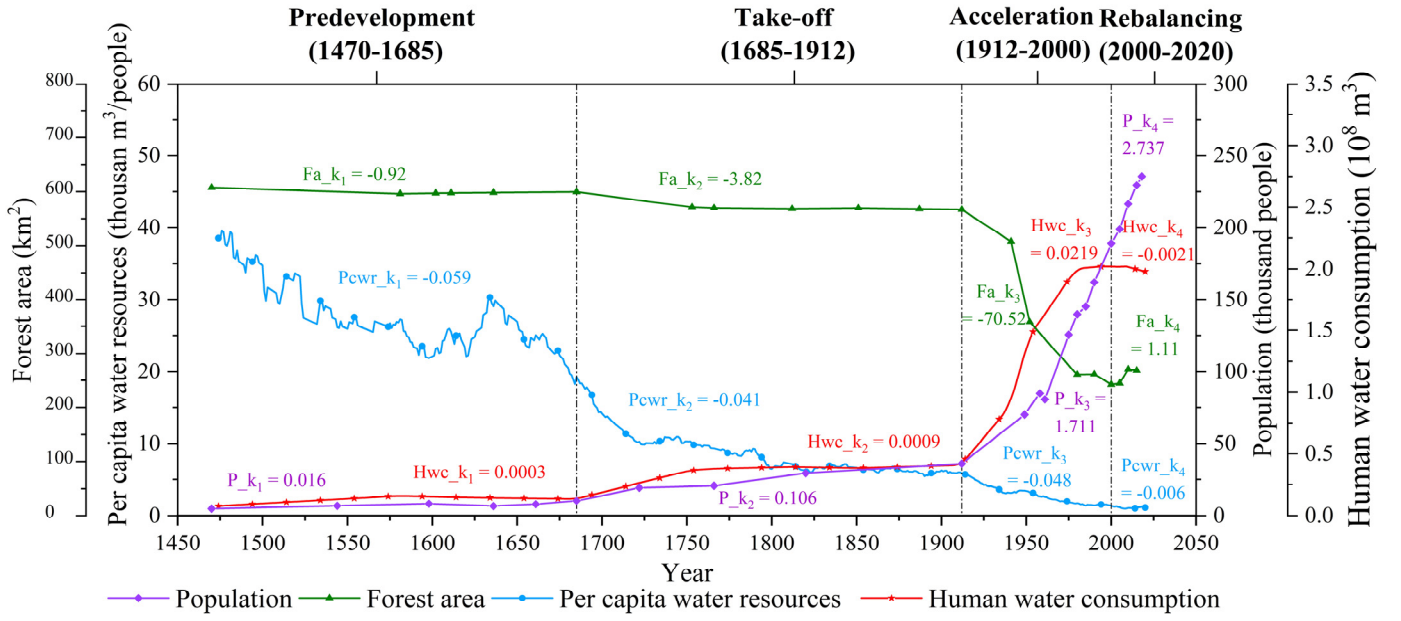


Figure 5. Division of the evolution stages of the HWR from 1470 to 2020. The per capita water resources and human water consumption are shown as 10-year moving averages.

5 Discussion

5.1 Why has the water cycle process remained stable at the village scale over the past six centuries?

Although the population and construction land area of “Baojia Tun” have been growing continuously over the past 600 years, the socioeconomic development mode is mainly a small-scale peasant economy, resulting in the water cycle structure remaining basically stable. Human water consumption is still dominated by irrigation water, but the percentages of the various elements in the water cycle process in the precipitation have changed (Fig. 2). From the LUCC of the whole basin, the cultivated land area in the basin has increased significantly since 1470 (the Ming Dynasty). Except for the large-scale expansion of construction land around cities and towns after 2000, the LUCC around other small residential areas are similar to those around “Baojia Tun”, so the socioeconomic development mode in the basin is still dominated by a small-scale peasant economy. Therefore, it can be inferred that the mode of human influence on the water cycle process in the basin has not changed, and the water cycle process in “Baojia Tun” can be extended to the study of the evolution of HWR at the basin scale.

The main reasons why the water cycle process in the “Tunpu” area has generally remained stable include natural factors and cultural factors. Among them, the natural factors are mainly related to the fact that the “Tunpu” area, Yangchang River basin, is located in the Anshun Plain, with open terrain, fertile soil and excellent climatic conditions. “There is seldom hot summer and cold winter”, which is suitable for the growth of crops. Therefore, the “Tunpu” area has always been an important grain production region in Guizhou Province (Chen, 2016). The specific cultural factors that are mainly present the “Tunpu”

culture itself have academic study value and cultural value. To fully protect the “Tunpu” villages, the local government mainly focuses on the development and construction of industries such as culture and tourism by using “Tunpu” villages, which leads to the fact that the socioeconomic development mode of the entire basin is still dominated by a small-scale peasant economy, and no large-scale industrial developments have been carried out (Chen, 2018).

5.2 What are the driving forces of the runoff changes at the basin scale?

From 1470 to 2020, under the joint impacts of climate change and human activities, the runoff trend changed from a slow decrease to an accelerated increase, and the rate of change increased from $-0.073 \times 10^4 \text{ m}^3 \cdot \text{a}^{-1}$ in the Ming Dynasty (1470-1636) to $30.946 \times 10^4 \text{ m}^3 \cdot \text{a}^{-1}$ in the China period (e.g., 1949-2020) (Fig. 3). Regarding climate change, precipitation has the greatest impact on runoff, and there is an obvious positive correlation between precipitation and runoff ($R^2 = 0.86$), which is consistent with the existing research conclusions (Yuan et al., 2019; Jiang et al., 2021). In addition, human activities can be divided into irrigation water intake and LUCC. To determine the extent of the impacts of different human activities on the water cycle process, runoff calculations under the influence of different human activities can be conducted by controlling the land use/cover or irrigation water volume (Fig. 6).

Fig. 6 shows that the increased runoff in the basin results from the offsetting impacts of two different human activities on the water cycle process, and the increased runoff caused by LUCC is greater than the decreased runoff caused by irrigation water intake. Under the scenario of only considering the LUCC, from 1470 to 2020, the change rate of runoff increased significantly from $4.41 \times 10^4 \text{ m}^3 \cdot \text{a}^{-1}$ to $14.8 \times 10^4 \text{ m}^3 \cdot \text{a}^{-1}$. Meanwhile, the LUCC in each stage lead to runoff increases, but their impacts are different: from the predevelopment to acceleration stage, the degree of impact of the LUCC gradually increases from 2.10% to 32.26%, and the LUCC modes consist mainly of the transformation from forestland to cultivated land, which will reduce the total evapotranspiration during this period and increase the runoff (Du et al., 2018). In the rebalancing stage, the impact degree of the LUCC in the rebalancing stage is only 22.82%, and the main LUCC modes consist of the expansion of construction land and restoration of forestland, which will significantly increase the runoff levels due to the impermeability of construction land and the increased evapotranspiration of forestland (Zhao et al., 2016).

Then, under a scenario that considers both LUCC and irrigation at the same time, from 1470 to 2020, the change rate of runoff decreased significantly from $14.8 \times 10^4 \text{ m}^3 \cdot \text{a}^{-1}$ to $8.41 \times 10^4 \text{ m}^3 \cdot \text{a}^{-1}$. It can be also found that irrigation always causes reductions in runoff, and the impact of irrigation gradually increased from -1.72% in the predevelopment stage to -18.97% in the rebalancing stage due to the continuous increase in the average cultivated land area.

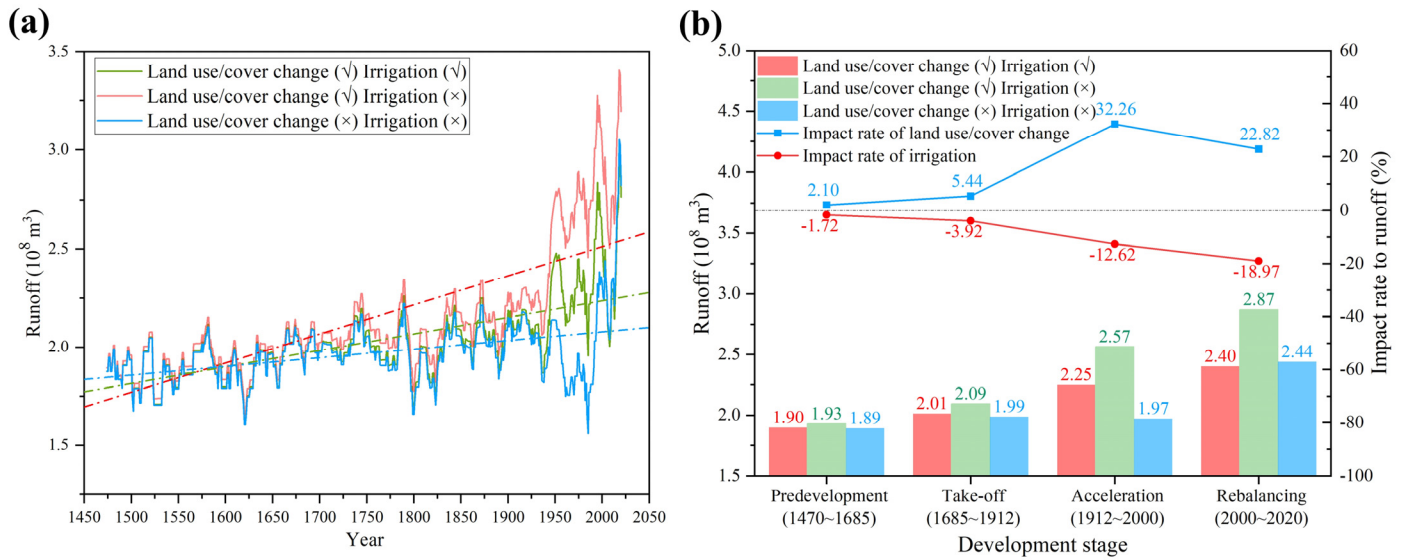


Figure 6. (a) Runoff under the influence of different human activities; and (b) impact rate of different human activities on the runoff.

5.3 How does the policy rebuild HWR?

The HWR that developed from the initial balanced resource-rich period to the unbalanced period of extensive development finally began to transform to the rebalancing period after 2000 (Fig. 5). The reason for the rebalancing of HWR is mainly because China recognizes that the extensive development mode is unsustainable and needs to complete the transformation from an industrial civilization to the ecological civilization (Pan, 2012; Lu et al., 2019). In this regard, Guizhou Province, where the “Tunpu” area is located, has responded positively and taken a series of measures. For example, in 2000, Guizhou Province vigorously promoted an ecological construction project that focused on the Grain for Green project. In 2007, it established a strategy of “building a province with environment” and took the lead in making the strategic decision of building the ecological civilization in China. In 2012, the construction of an important ecological security barrier in the upper reaches of the “two rivers” will be one of the five strategic positions of Guizhou in the future. In 2016, Guizhou Province was established as a national ecological civilization pilot area (Jiang et al., 2014). These policies are not just slogans or visions but are real ongoing processes (Pan, 2012).

Taking the earliest Grain for Green project as an example, since its launch in 2000, Guizhou Province has completed the task of the Grain for Green project of 204.72 thousand km², and the forest coverage rate in the entire province has increased from 22.8% in 1975 to 59.95% in 2020. The value of the annual ecological benefit that was created by the Grain for Green project reached 84.072 billion yuan. The soil erosion modulus decreased from 3325 tons per km²·a⁻¹ in 2000 to 631.4 tons per km²·a⁻¹ in 2017, which was 72% lower than that before the Grain for Green project (Xiao et al., 2015; Zhang & Yang, 2021). By combining satellite remote sensing (MOD13A1.006 Terra Vegetation Indices, 500 m), aerial remote sensing and unmanned aerial vehicle remote sensing, we can more clearly observe that the Yangchang River basin is turning green (Fig. 7). For the

entire basin, the average Normalized Difference Vegetation Index (NDVI) exhibited an obvious upwards trend with a rate of 0.002/year from 2001 to 2020 ($P < 0.05$), which indicates that the entire basin is turning green, which is consistent with the previous land use/cover results and relevant policies. In terms of the spatial distribution, the NDVIs of 79.04% of the areas in the basin exhibit an increasing trend and are mainly distributed in the middle and south portions of the basin. The land use/cover types in these areas consist mainly of cultivated land, forest and grassland, which are the main areas for the Grain for Green project. By comparing the aerial remote sensing images and unmanned aerial vehicle remote sensing images of areas (a) and (b) shown in Fig. 8, it is clear that the conversion from sloping farmland to forestland has significantly improved the level of forestland coverage. Meanwhile, the remaining 20.96% of the areas with decreased NDVIs are mainly distributed near the large cities and towns in the basin, where the expansion of construction land was concentrated in the basin from 2001 to 2020. However, the transformation from cultivated land to forestland can still be clearly found in the images of areas (c) and (d), as shown in Fig. 8. At the same time, the low-coverage grasslands on the mountains are also changing to forestland with high coverage. This demonstrates that whether in natural areas or areas with human activities, while promoting socioeconomic development, the entire basin is also paying attention to restoring the ecological environment. The ecological civilization can rebuild HWR and cause it to gradually transition to a rebalancing stage from 2000 to 2020, which is similar to the conclusions of studies of the Tarim River Basin (Liu et al., 2014), Heihe River Basin (Lu et al., 2015) and Loess Plateau (Wu et al., 2020).

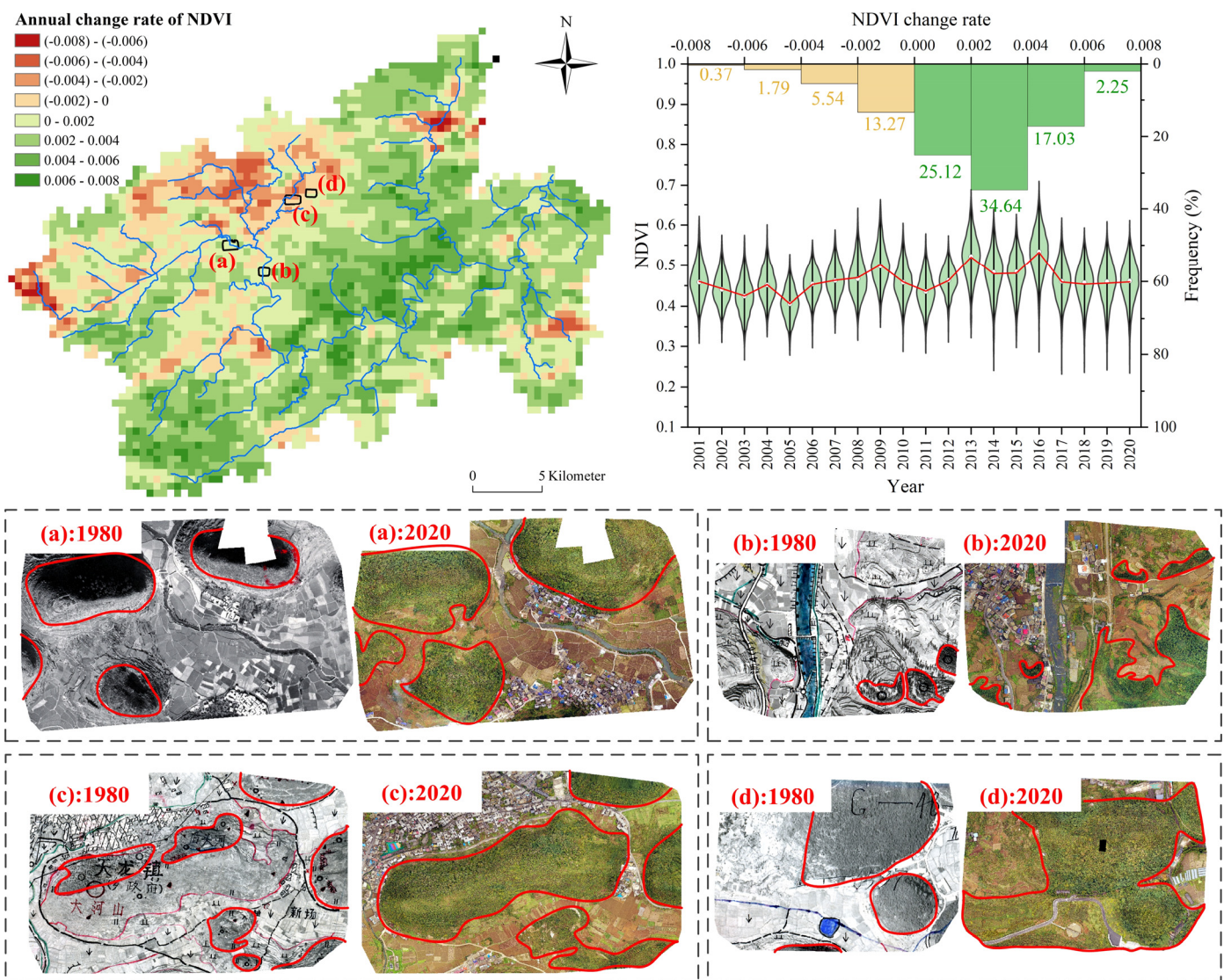


Figure 7. Vegetation restoration under the Grain for Green project in the rebalancing stage. The area outlined by the red line is the approximate area of vegetation growth.

5.4 Validation of the method for reconstructing water cycle process over the past 600 years

The water cycle process at the basin scale in the past 600 years is reconstructed, and then the reliability analysis will be carried out from the perspective of runoff and precipitation. Firstly, based on RSHS and multi-source remote sensing data (Landsat-7, Landsat-8, Sentinel-1, Sentinel-2), the digital river model was constructed (Fig.8a and 8b) and the surface runoff from 2001 to 2020 was calculated, and then compared with the reconstructed runoff from 2001 to 2020 (Fig.8c). It can be found in Fig.6a-c that the accuracy of surface runoff estimated by RSHS is reliable. The multi-year average runoff calculated by RSHS and water balance formula is relatively close, which are 2.80 and $2.37 \times 10^8 \text{ m}^3$, respectively. Besides, through the correlation analysis chart, it can be found that there is an obvious positive correlation between the two ($R^2 = 0.61$, $P < 0.05$), indicating that the flow calculated by the water balance formula has the same change trend as the surface runoff calculated by

RSHS, which can reflect the change trend of water resources in the basin to a certain extent. Nevertheless, the total runoff calculated by the water balance formula fluctuates greatly and is sometimes less than the surface runoff calculated by RSHS. This is mainly because the water balance formula ignores the interannual water storage change of the basin by setting the water storage variables of the basin to 0 for every year.

Then, by comparing the measured precipitation and the precipitation simulated by the drought and flood level distribution map in *Atlas of drought and flood distribution in China in recent 500 years* from 1959 to 2000 (Fig.8d), it can be found that there is a good positive correlation between them, and the Nash efficiency coefficient reaches 0.57. Meanwhile, in the graph of correlation analysis, all points are distributed around the 1:1 line, the slope of linear fitting is 0.93, and $R^2 = 0.62$. This shows that using the drought and flood levels in the atlas to simulate the precipitation in historical periods is reliable, and the precipitation corresponding to each drought and flood level is set reasonably.

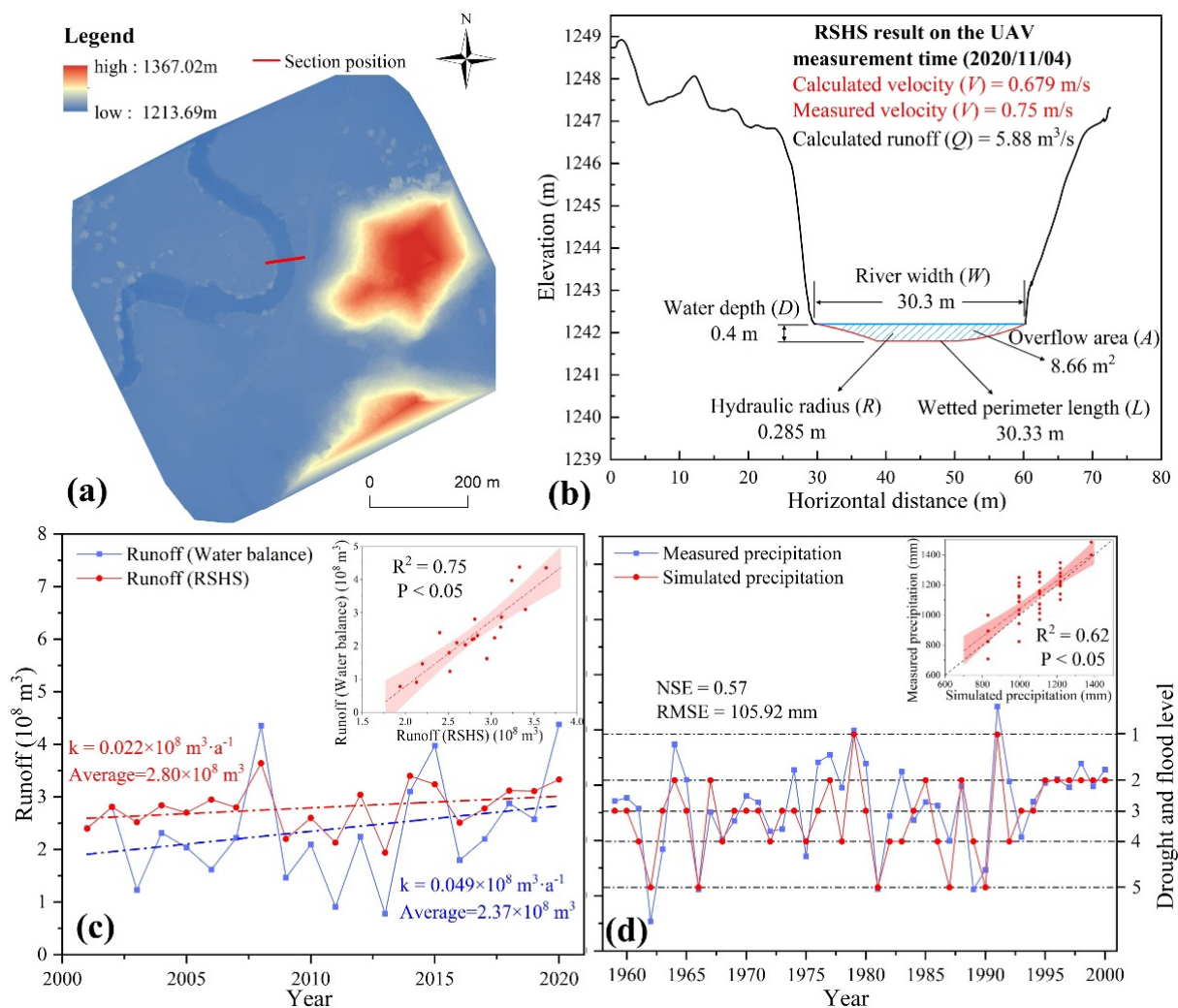


Figure 8. Reliability analysis of runoff and precipitation. (a) Digital Surface Model and section position; (b) river cross section elevation and hydraulic parameter result of the UAV measurement time (2020/11/04); (c) comparison between surface runoff calculated by RSHS and the runoff calculated by the water balance formula; and (d) comparison between measured precipitation and simulated precipitation.

6 Conclusion

By combining the historical literature, statistical data and multisource remote sensing data and taking the “Tunpu” area, Yangchang River Basin with a 600-year history of water resource development in Guizhou, China, as a typical study area, this research analyses the evolution of the HWR in different space and time spans over the past 600 years based on the RSHS technology and an improved water balance formula. Then, based on transition theory, the key time nodes in the evolution of HWR are determined, and the impacts of the ecological civilization on the HWR are analysed. The main conclusions are as follows:

At the village scale, the water cycle structure of the typical villages remained mostly stable from the Ming Dynasty to modern times, and the deforestation that was caused by the expansion of towns and cultivated land increased the proportion of runoff in precipitation by 10.62%. At the basin scale, the runoff trend changed from a slow decrease to an accelerated increase from 1470 to 2020, and the change rate increased from $-0.073 \times 10^4 \text{ m}^3 \cdot \text{a}^{-1}$ in the Ming Dynasty (1470-1636) and gradually increased to $30.946 \times 10^4 \text{ m}^3 \cdot \text{a}^{-1}$ in the China stage (e.g., 1949-2020), which was due to the LUCC transformations from cultivated land expansion to construction land expansion and forestland restoration, as well as the impact of fluctuating precipitation increases. The HWR have developed from the balanced initial resource-rich period to the unbalanced period of extensive development, and have finally transformed into a rebalancing period under the influence of the ecological civilization policy. The four stages are as follows: predevelopment (1470-1685), take off (1685-1912), acceleration (1912-2000) and rebalancing (2000-2020).

This research indicates that the ecological civilization policy can rebuild HWR and cause a transition to the rebalancing stage, and this policy is expected to provide enlightenment for future water resource management efforts and for the construction of the ecological civilization to further achieve the harmonious development of humans and water. Also, in addition to irrigation water and domestic water, factors such as warfare, human beliefs and consciousness that are proposed in the social sciences can affect the evolution of HWR, which need to be conducted in future studies.

References

- Ahmad, I., Waseem, M., Lei, H., et al., 2018. Harmonious level indexing for ascertaining human-water relationships. *Environmental Earth Sciences*. 77(4). <https://doi.org/10.1007/s12665-018-7296-7>
- Bao, C., & Zou, J., 2018. Analysis of spatiotemporal changes of the human-water relationship using water resources constraint intensity index in Northwest China. *Ecological Indicators*. 84, 119-129. <https://doi.org/10.1016/j.ecolind.2017.08.056>
- Cai, Y., Peng, Z., An, Z., et al., 2001. Oxygen isotope records of Holocene stalagmites in qixingdong, Guizhou and their indication of monsoon climate change. *Scientific Bulletin*.(16), 1398-1402. (in Chinese).
- Ceola, S., Montanari, A., Krueger, T., et al., 2016. Adaptation of water resources systems to changing society and environment: a statement by the International Association of Hydrological Sciences. *Hydrological Sciences Journal-Journal Des Sciences*

Hydrologiques. 61(16), 2803-2817. <https://doi.org/10.1080/02626667.2016.1230674>

Chen, J. (2016). *The development and changes of agriculture in Anshun during the Ming and Qing Dynasties*. Guizhou Normal University. (in Chinese).

Chen, Y., 2018. Study on the protection and inheritance of Tunpu culture in Anshun. *Theory and Contemporary*.(11), 59-61. (in Chinese).

Du, L. Y., Rajib, A., & Merwade, V., 2018. Large scale spatially explicit modeling of blue and green water dynamics in a temperate mid-latitude basin. *Journal of Hydrology*. 562, 84-102. <https://doi.org/10.1016/j.jhydrol.2018.02.071>

Falkenmark, M., 2001. The greatest water problem: The inability to link environmental security, water security and food security. *International Journal of Water Resources Development*. 17(4), 539-554. <https://doi.org/10.1080/07900620120094073>

Fu, B.-P., 1981. On the calculation of the evaporation from land surface. *Chinese Journal of Atmospheric Sciences*. 5, 23-31. (in Chinese).

Hansen, M. H., Li, H. T., & Svarverud, R., 2018. Ecological civilization: Interpreting the Chinese past, projecting the global future. *Global Environmental Change-Human and Policy Dimensions*. 53, 195-203. <https://doi.org/10.1016/j.gloenvcha.2018.09.014>

Institute of Meteorological Sciences, C. M. A., 1981. Atlas of drought and flood distribution in China in recent 500 years. Map publishing house.

Jiang, C., Wang, Z., & Huang, W., 2014. Status of Ecological Civilization Construction in Guizhou Province and Countermeasures. *China Environmental Monitoring*.(3), 13-17. <https://doi.org/10.3969/j.issn.1002-6002.2014.03.004> (in Chinese).

Jiang, D., 1982. Population survey of Guizhou in the early Qing Dynasty. *Guizhou Social Sciences*.(4), 50-54. (in Chinese).

Jiang, J. C., Lyu, L. T., Han, Y. C., et al., 2021. Effect of Climate Variability on Green and Blue Water Resources in a Temperate Monsoon Watershed, Northeastern China. *Sustainability*. 13(4), 2193. <https://doi.org/10.3390/su13042193>

Leitholdt, E., Zielhofer, C., Berg-Hobohm, S., et al., 2012. Fossa Carolina: The First Attempt to Bridge the Central European Watershed-A Review, New Findings, and Geoarchaeological Challenges. *Geoarchaeology-an International Journal*. 27(1), 88-104. <https://doi.org/10.1002/gea.21386>

Li, K., & Xu, Z. F., 2006. Overview of Dujiangyan Irrigation Scheme of ancient China with current theory. *Irrigation and Drainage*. 55(3), 291-298. <https://doi.org/10.1002/ird.234>

Li, Y., Li, H., Li, D., et al., 2020. Construction of rural water ecological civilization index system in China. *Water Practice and Technology*. 15(3), 797-806. <https://doi.org/10.2166/wpt.2020.064>

Liu, D., Tian, F., Lin, M., et al., 2015. A conceptual socio-hydrological model of the co-evolution of humans and water: case study of the Tarim River basin, western China. *Hydrology and Earth System Sciences*. 19(2), 1035-1054. <https://doi.org/10.5194/hess-19-1035-2015>

Liu, H., & Wang, L., 2018. Construction of Urban Water Ecological Civilization System. *IOP Conference Series: Earth and Environmental Science*. 170, 032111. <https://doi.org/10.1088/1755-1315/170/3/032111>

Liu, Y., Tian, F., Hu, H., et al., 2014. Socio-hydrologic perspectives of the co-evolution of humans and water in the Tarim River basin, Western China: the Taiji-Tire model. *Hydrology and Earth System Sciences*. 18(4), 1289-1303. <https://doi.org/10.5194/hess-18-1289-2014>

Lou, H. Z., Wang, P. F., Yang, S. T., et al., 2020. Combining and comparing an Unmanned Aerial Vehicle and multiple remote sensing satellites to calculate long-term river discharge in an ungauged water source region on the Tibetan Plateau. *Remote Sensing*. 12(13), 2155. <https://doi.org/10.3390/rs12132155>

Lu, Y., Zhang, Y., Cao, X., et al., 2019. Forty years of reform and opening up: China's progress toward a sustainable path. *Sci. Adv*. 5(8), eaau9413. <https://doi.org/doi:10.1126/sciadv.aau9413>

Lu, Z., Wei, Y., Xiao, H., et al., 2015. Evolution of the human-water relationships in the Heihe River basin in the past 2000 years. *Hydrology and Earth System Sciences*. 19(5), 2261-2273. <https://doi.org/10.5194/hess-19-2261-2015>

Nie, Z., 2017. Anshun Tunbao: here, I found the Ming Dynasty. *Tong Zhou Gong Jin* (09), 72-76. <https://doi.org/10.19417/j.cnki.tzgj.2017.09.020> (in Chinese).

Pan, J., 2012. From Industrial Toward Ecological in China. *Science*. 336(6087), 1397-1397. <https://doi.org/doi:10.1126/science.1224009>

- Pan, Y. (2021). *Study on the evolution of spatial form of typical Tunpu settlements in Anshun*. Guizhou Normal University. (in Chinese).
- Ren, C., Lu, Y., & Yang, D., 2010. Drought and flood disasters and rebuilding of precipitation sequence in Heihe River Basin in the past 2000 years. *Journal of arid land resources and environment*. 24(06), 91-95. <https://doi.org/10.13448/j.cnki.jalre.2010.06.009> (in Chinese).
- Sha, F., & Iop. (2018, Dec 07-09). *The predicament and realization path of China's eco-civilization construction*. 4th International Conference on Advances in Energy Resources and Environment Engineering (ICAEESEE), Chengdu, PEOPLES R CHINA.
- Sheng, Y., Zeng, M., Peng, H., et al., 2019. Reconstruction and Analysis of Dry/Wet Series in Guizhou Area in 1470-1949. *Resources and Environment in the Yangtze Basin*. 28(6), 1354-1364. <https://doi.org/10.11870/cjlyzyyhj201906011> (in Chinese).
- Sivapalan, M., Savenije, H. H. G., & Blöschl, G., 2012. Socio-hydrology: A new science of people and water. *Hydrological Processes*. 26(8), 1270-1276. <https://doi.org/10.1002/hyp.8426>
- Tàbara, J., & Ilhan, A., 2008. Culture as trigger for sustainability transition in the water domain: The case of the Spanish water policy and the Ebro river basin. *Regional Environmental Change*. 8(2), 59-71. <https://doi.org/10.1007/s10113-007-0043-3>
- Tian, P., Wu, H. Q., Yang, T. T., et al., 2021. Evaluation of urban water ecological civilization: A case study of three urban agglomerations in the Yangtze River Economic Belt, China. *Ecological Indicators*. 123. <https://doi.org/10.1016/j.ecolind.2021.107351>
- Wang, J., Wei, Y., Jiang, S., et al., 2017. Understanding the Human-Water Relationship in China during 722 BC-1911 AD from a Contradiction and Co-Evolutionary Perspective. *Water Resources Management*. 31(3), 929-943. <https://doi.org/10.1007/s11269-016-1555-8>
- Wang, P. F., Yang, S. T., Wang, J., et al., 2020. Discharge estimation with hydraulic geometry using unmanned aerial vehicle and remote sensing. *Journal of Hydraulic Engineering*. 51(04), 492-504. <https://doi.org/10.13243/j.cnki.slxb.20190742> (in Chinese).
- Wu, X. T., Wei, Y. P., Fu, B. J., et al., 2020. Evolution and effects of the social-ecological system over a millennium in China's Loess Plateau. *Sci. Adv.* 6(41). <https://doi.org/10.1126/sciadv.abc0276>
- Wufu, A., Chen, Y., Yang, S. T., et al., 2021. Changes in Glacial Meltwater Runoff and Its Response to Climate Change in the Tianshan Region Detected Using Unmanned Aerial Vehicles (UAVs) and Satellite Remote Sensing. *Water*. 13(13), 1753. <https://doi.org/10.3390/w13131753>
- Xiao, L. G., & Zhao, R. Q., 2017. China's new era of ecological civilization. *Science*. 358(6366), 1008-1009. <https://doi.org/10.1126/science.aar3760>
- Xu, X., Liu, J., Zhang, S., et al., 2018. China multi period land use and land cover remote sensing monitoring data set(CNLUCC).Data registration and publishing system of resource and environmental science data center of Chinese Academy of Sciences (<http://www.resdc.cn/DOI>), DOI:10.12078/2018070201).
- Xue, C., Xiaobin, J., Wang, J., et al., 2014. Reconstruction and change analysis of cropland data of China in recent 300 years. *Journal of Geography*. 69(7), 896-906. <https://doi.org/10.11821/dlxb201407002> (in Chinese).
- Yang, B., 1996. Analysis of Guizhou population data in the early Qing Dynasty. *Chinese Population Science*.(4), 50-54. (in Chinese).
- Yang, Q., Gao, D., Song, D., et al., 2021. Environmental regulation, pollution reduction and green innovation: The case of the Chinese Water Ecological Civilization City Pilot policy. *Economic Systems*. 45(4). <https://doi.org/10.1016/j.ecosys.2021.100911>
- Yang, S., Wang, P., Wang, J., et al., 2021. River Flow Estimation Method Based on UAV Aerial Photogrammetry. *Journal of Remote Sensing*. 25(6), 1284-1293. <https://doi.org/10.11834/jrs.20209082> (in Chinese).
- Yang, S. T., Li, C. J., Lou, H. Z., et al., 2020. Performance of an Unmanned Aerial Vehicle (UAV) in calculating the flood peak discharge of ephemeral rivers combined with the incipient motion of moving stones in arid ungauged regions. *Remote Sensing*. 12(10), 1610. <https://doi.org/10.3390/rs12101610>
- Yang, S. T., Wang, P. F., Lou, H. Z., et al., 2019. Estimating river discharges in ungauged catchments using the slope-area method and Unmanned Aerial Vehicle. *Water*. 11(11), 2361. <https://doi.org/10.3390/w11112361>
- Yuan, Z., Xu, J. J., Meng, X. Y., et al., 2019. Impact of Climate Variability on Blue and Green Water Flows in the Erhai Lake Basin of Southwest China. *Water*. 11(3), 424. <https://doi.org/10.3390/w11030424>
- Zhang, D., Li, X., & Liang, Y., 2003. A further supplement to the atlas of drought and flood distribution in China in recent 500 years

(1993-2000). Journal of Applied Meteorology. 14(3), 10. (in Chinese).

Zhang, D., & Liu, C., 1993. Continuation of Atlas of drought and flood distribution in China in recent 500 years (1980-1992). Meteorology. 19(11), 5. (in Chinese).

Zhang, M., Liu, Y. M., Wu, J., et al., 2018. Index system of urban resource and environment carrying capacity based on ecological civilization. Environmental Impact Assessment Review. 68, 90-97. <https://doi.org/10.1016/j.eiar.2017.11.002>

Zhang, W., & Pang, Y., 2007. Investigation of 600 years of water use in Baotun. China Water Resources.(12), 51-55. <https://doi.org/10.3969/j.issn.1000-1123.2007.12.026> (in Chinese).

Zhang, X., 1998. The impact of Guizhou's population development on social economy in the Ming and Qing Dynasties. Journal of Guizhou Normal University (Social Sciences Edition).(3), 21-25. (in Chinese).

Zhao, A. Z., Zhu, X. F., Liu, X. F., et al., 2016. Impacts of land use change and climate variability on green and blue water resources in the Weihe River Basin of northwest China. Catena. 137, 318-327. <https://doi.org/10.1016/j.catena.2015.09.018>

Zhao, C., Pan, X., Yang, S., et al., 2019. Measuring streamflow with low-altitude UAV imagery. Acta Geographica Sinica. 74(7), 1392-1408. <https://doi.org/10.11821/dlxb201907009> (in Chinese).

Zhao, K. (2011). *Stalagmite laminar chronology and isotopic climate reconstruction in donggedong, Guizhou Province in recent 1000 years*. Nanjing Normal University. (in Chinese).

Zhao, W., Ding, J., Wang, Y., et al., 2020. Ecological water conveyance drives human-water system evolution in the Heihe watershed, China. Environmental Research. 182. <https://doi.org/10.1016/j.envres.2019.109009>

Zhou, Z., & Xu, J., 2018. Study on Water Environment and Water Landscape in Tunpu Villages in Anshun, Guizhou Province. Journal of Western Human Settlements.(1), 101-106. <https://doi.org/10.13791/j.cnki.hsfwest.20180116> (in Chinese).

Zuo, Q., Diao, Y., Hao, L., et al., 2020. Comprehensive Evaluation of the Human-Water Harmony Relationship in Countries Along the "Belt and Road". Water Resources Management. 34(13), 4019-4035. <https://doi.org/10.1007/s11269-020-02632-2>

Zuo, Q., Li, W., Zhao, H., et al., 2021. A Harmony-Based Approach for Assessing and Regulating Human-Water Relationships: A Case Study of Henan Province in China. Water. 13(1). <https://doi.org/10.3390/w13010032>

Acknowledgement

The authors thank the National Natural Science Foundation of China (Grant Nos. U1812401, 41801293) and the Key Project of Philosophy and Social Sciences Planning in Guizhou Province (19GZZD07), the Open Research Fund Program of State Key Laboratory of Hydro-science and Engineering (sklhse-2021-A-04), and the Fundamental Research Funds for the Central Universities (2017NT11). We also thank the AJE group for editing the English text of a draft of this manuscript.

Data availability statement

The data that supports the findings of this study are available in the supplementary material of this article. Among them, excel files is the data in each figure, including calculated precipitation, evapotranspiration, runoff, land use/cover change statistics, etc. Remote sensing data include, land use/cover, NDVI, evapotranspiration.

Author contribution

S.Y. contributed to methodology, software, review and editing, supervision, project administration and funding acquisition.

611 H.L. contributed to methodology, software, writing, calculation, review and editing and supervision. Z.P. contributed to
612 methodology, data curation, calculation, visualization, writing. C.L., J.Z., and Y.Z. contributed to data curation, validation.
613 Y.Y., J.G., Y.L., and X.L. contributed to data provision and supervision.
614

615 **Competing interests**

616 The authors declare no competing interests.